Appl. Phys. A 91, 379–383 (2008)
DOI: 10.1007/s00339-008-4439-9

Applied Physics A
Materials Science & Processing

S.P. DASH
D. GOLL
H.D. CARSTANJEN✉

Near-surface compositional oscillations of Co diffused into Si(100) at −60 °C: a study by high-resolution Rutherford backscattering

Max-Planck-Institut für Metallforschung, Heisenbergstraße 3, 70569 Stuttgart, Germany

Received: 14 November 2007 / Accepted: 30 January 2008
Published online: 6 March 2008 •

ABSTRACT Highly resolved Co depth profiles have been obtained during the initial stages of Co growth on Si(100) at low temperature (−60 °C) by in situ high-resolution Rutherford backscattering spectrometry. We found extensive Co in-diffusion in the submonolayer growth regime even at this low temperature, besides Co on top of the Si surface. The amount of diffused-in Co is larger than the amount of Co at the Si surface. Every second Si layer is depleted of Co, starting at the Si surface, thus giving rise to compositional oscillations of Co in the Si(100) lattice. At this low temperature the growth of metallic Co on the Si surface is observed at 0.1 ML of deposited Co, which continues for higher coverages. At much higher coverage (5.93 ML of Co) almost exclusively low Co content silicides are formed at the Co/Si interface. The data presented here are compared with previous room temperature deposition data and are different in several aspects.

PACS 68.35.-p; 68.55.ag; 75.47.-m; 82.80.Yc

1 Introduction

Exploiting the spin of the electron in addition to its charge to explore a new generation of spintronic devices which will be smaller, more versatile and more robust than those currently making up silicon chips has both fundamental and technological importance [1, 2]. High spin polarization of Co at room temperature (∼ 40%) [3] and a long spin coherence length in Si (longer than micrometers) [4] make the materials Co and Si attractive for spin-injection experiments. In such a heterostructure of a Co thin film on a Si substrate, any structural disorder at the interface would drastically reduce the spin polarization at the interface and, hence, the spin-injection efficiency [5–8]. If a small amount of Co diffuses into the Si, each such Co atom will be likely to carry a local magnetic moment oriented randomly with respect to the magnetization direction of the Co thin film. They will scatter the injected spin polarized electrons, thereby degrading their spin polarization [8]. Thus, in order to control and improve the properties of the interface, a detailed understanding of its structure is necessary.

As understood from the growth of Co on Si(100) at room temperature, diffused-in Co atoms occupying the tetrahedral interstitial sites are the main cause for the weakening of Si–Si bonds [9–16]. These weakened bonds allow Si atoms to diffuse out to the surface and form silicide-like phases. Thus, any experimental measure to prohibit the diffusion of Co into the Si lattice would reduce the formation of silicide.

In this article, we therefore investigated the Co depth distribution and Co/Si composition at the initial stages of Co growth on Si(100) in an in situ experiment by high-resolution Rutherford backscattering spectrometry (HRBS) [17] at low temperature (−60 °C). From a RUMP [18] fitting of our experimental results we obtained information about the main diffusing species, the thickness of the reacted Si layer and the different phases formed at −60 °C from very initial stages to fully metallic Co coverage.

2 Experiment

The in situ HRBS measurements were performed in an ultra-high-vacuum (UHV) system consisting of a preparation chamber, connected to a Pelletron accelerator, and an electrostatic spectrometer [17] for energy analysis of scattered 2-MeV N^+ ions at an incidence angle of 2° to the sample surface and at a scattering angle of 37.5°. These angles are far enough away from major crystal axes so that ion-channeling effects can be ruled out (critical angles of axial channeling are of the order of 0.85°). In the analysis, scattered N^{3+} ions were used. Their charge state 3 is very close to the equilibrium charge state of scattered N ions at the energies used in the experiment and in this way artifacts are avoided which can occur when non-equilibrium charge states (e.g. 1 or 5) are used. The energy resolution of the detector is 4 keV for the present case, which corresponds to 1-Å depth resolution in Si and 0.5-Å depth resolution in Co. Chemically cleaned n-Si(100) samples with resistivity of 4–10 Ω cm (P-doped) were further cleaned in UHV by flash

✉ Fax: +49-711-689-1977, E-mail: carstanjen@mf.mpg.de

heating at 950 °C. From this temperature the samples were slowly cooled to −60 °C. The surface cleanness of the Si samples was verified by HRBS measurements. In the experiment, both the Co growth (0.1 to 5.93 ML, 1 ML = 6.87×10^{14} atoms/cm^2 = number density of Si(100) layers) and the HRBS measurements were done keeping the Si substrate at −60 °C. Co with 4 N purity was evaporated from an effusion cell. Before use the effusion cell was outgassed; no C or O contaminants were found during evaporation. The evaporation rate (0.05 ML/min) was calibrated by HRBS with an accuracy of about 5%. Each HRBS spectrum was taken on a new spot (size ∼ 1 mm^2) to minimize the influence of radiation damage.

3 Results and discussion

The HRBS spectrum of the Co distribution for the coverage of 0.1 ML is shown in Fig. 1a. The spectrum shows three distinct peaks, which correspond to Co atoms in three well-defined depths in the Si lattice: at the surface, below the surface and somewhat further inside. In order to obtain more detailed information about the Co depth distribution, the Co spectrum was simulated by the program RUMP [18]. In these simulations the Si sample was subdivided into thin sublayers containing exactly 6.87×10^{14} /cm^2 Si atoms and the appropriate amount of Co atoms added up. The composition of each sublayer was varied (by varying the Co content) and the HRBS spectrum calculated for the assumed Co depth distribution until good agreement was achieved with the experimental data. At the small coverages of Fig. 1a and also Fig. 2a (0.1–1.3 ML), the Co atoms were assumed to be adsorbed on top of the Si surface and to occupy sites in the (100) Si layers, exclusively. The latter follows the results of Meyerheim et al. [9], indicating that at low Co coverage the Co atoms take tetrahedral interstitial sites in the Si lattice and four-fold hollow sites in the first Si layer, which all are allocated on (100) Si planes. We would like to note that we can exclude the growth of islands during Co deposition: from an Auger study, Gallego et al. [16] derived layer-by-layer growth of Co with some Si intermixed during deposition at room temperature. Also, from the HRBS data themselves this can be excluded: when island growth occurs, shadowing effects would become visible in the spectra at glancing incidence, resulting in a 'rounding off' of the high-energy edge of the spectra [19]. No such effects are seen in our HRBS spectra. We can, however, not exclude clusters of Co which are incorporated inside the Si lattice. Most probably such clusters are present at very low coverage. In this case the concentrations given in the following are average concentrations of Co, averaged over the individual layers.

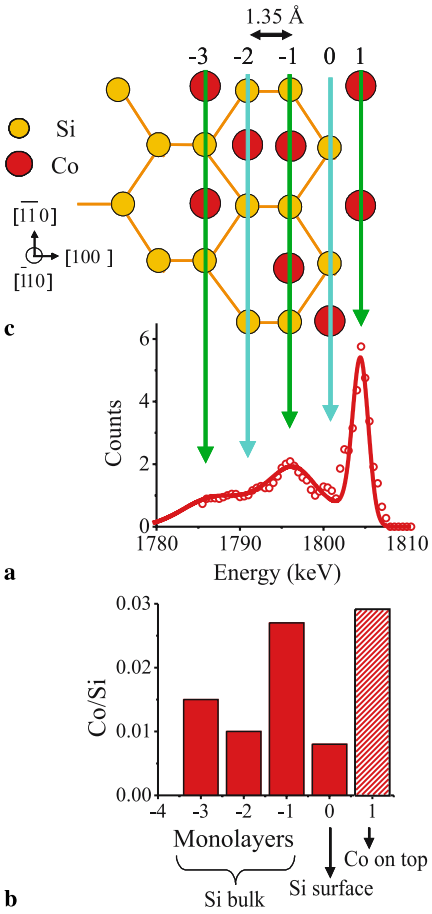

FIGURE 1 0.1 ML of evaporated Co on Si(100) at −60 °C. (**a**) Co edge of HRBS spectrum (*circles*) using 2-MeV N^+ ions and RUMP simulation (*solid line*). The peak at 1804 keV is due to backscattering from Co at the surface, the 2nd peak at 1796 keV is due to Co atoms in the −1st Si layer and the 3rd peak is due to Co atoms in the −3rd Si layer. (**b**) Co concentration (Co/Si) in the different Si(100) layers of the Si crystal as derived from the RUMP simulation. Each layer consists of 6.87×10^{14} Si atoms/cm^2 plus some Co atoms. Layer 1 (*hatched column*) corresponds to Co atoms growing on top of the Si crystal, layer 0 is the 1st Si layer; layers −1, −2 and −3 are subsequent layers in the Si bulk (*solid columns*). (**c**) Projected atomic positions of diffused Co atoms in the Si lattice showing atomic positions corresponding to the peaks of the HRBS spectrum

Figure 1b shows the Co concentration in the different sublayers as obtained from the RUMP simulation for 0.1 ML of Co coverage. According to these results the top-most layer is a layer of Co atoms on top of the Si surface (1st layer). As a careful analysis of our data shows, it is free of Si atoms (the presence of Si atoms in this layer would enter the RUMP simulation through a different stopping power). As Fig. 1a shows, we can fit our experimental data very well in this way, which we cannot do otherwise. It should be noted that this result is different from results for Co growth on Si(100) at room temperature by our group [13] (see also Fig. 2c) and by Meyerheim et al. [9], where only an incorporation of Co in the top-most Si layer was observed. The next layer, layer '0' in Fig. 1b, is the top-most (100) Si layer; it is almost free of Co. Layers −1, −2 and −3 are subsequent layers below the Si surface. They all exhibit small amounts of Co. This means that at a coverage as low as 0.1 ML, Co atoms have apparently diffused into the Si bulk up to the −3rd layer. The amount of diffused-in Co atoms is even higher than the amount of Co on top of the Si surface. The Co atoms are, however, by no means homogeneously distributed over this range. As Fig. 1b shows, every second Si layer is depleted of Co, thus giving an oscillatory Co distribution in the Si lattice. This is similar to the model for the diffusion microstructure of Ni in Si(100) by Chang and Erskine [20] and the distribution of metal atoms in metal alloys like Cu_3Au [21] close to the surface. A similar behavior is also observed for the growth of Fe on Si(100) at very low coverage at room temperature (to be published). In these systems such a configuration is stabilized by the minimization of the Gibbs free energy, consisting of atomic binding, strain and surface energies and the entropy of mixing.

Figure 1c finally illustrates the distribution of the Co atoms in the Si lattice and correlates this distribution with the peaks observed in the HRBS spectrum. The first peak at 1804 keV thus corresponds to Co atoms on top of the Si surface, the second peak at 1796 keV to Co atoms in the −1st layer (1.35 Å from the Si surface) and the third peak to Co atoms in the −3rd layer (4.05 Å from the Si surface).

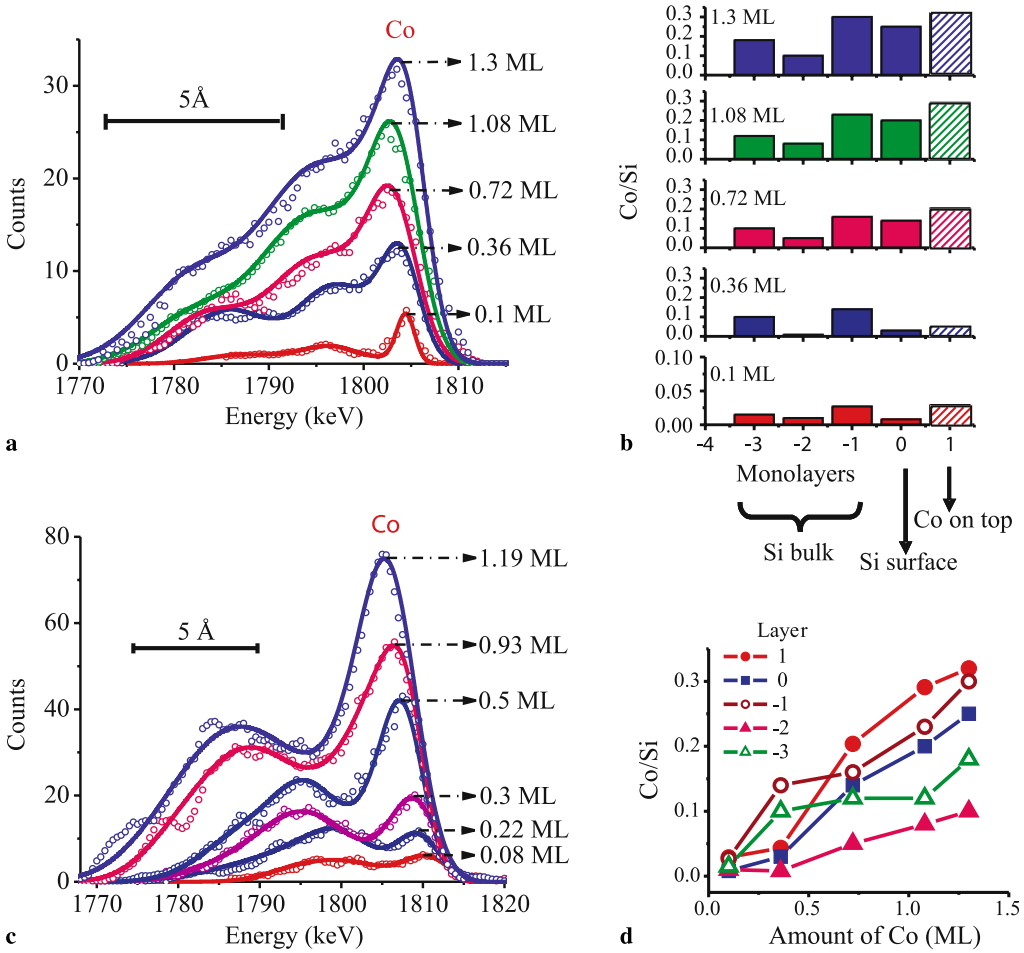

FIGURE 2 (**a**) Co on Si(100), submonolayer coverage (0.1 to 1.3 ML) at −60 °C: Co edge of HRBS spectra (*circles*) using 2-MeV N^+ ions and RUMP simulations (*solid lines*). (**b**) Co concentration (Co/Si) in the different Si(100) layers of the Si crystal as derived from (**a**) by RUMP simulations. Each layer consists of 6.87×10^{14} Si atoms/cm^2 plus some Co atoms. Layer 1 (*hatched column*) corresponds to Co atoms growing on top of the Si crystal, layer 0 is the 1st Si layer; layers −1, −2 and −3 are subsequent layers in the Si bulk (*solid columns*). Note: the *y* axis for 0.1 ML is scaled differently than the others. (**c**) HRBS spectrum of Co on Si(100) deposited at room temperature [13] (2-MeV N^+ ions, incidence angle 2.5°, submonolayer coverage 0.08–1.19 ML): experimental data (*circles*) and RUMP simulations (*solid lines*). The peaks between 1805 and 1815 keV are due to backscattering from Co at the surface. A second peak in the range of 1785–1800 keV is due to subsurface Co enrichment in the Si bulk. (**d**) Co concentration (Co/Si) in the layers −3 to +1 of Fig. 2b vs. the amount of evaporated Co (0.1 to 1.3 ML) on Si(100). As the figure shows, layers 0 and −2 are Co depleted compared to adjacent layers

With increasing coverage (from 0.36 to 1.3 ML) the amount of diffused-in Co increases, as does the amount of Co on top of the Si surface (see Fig. 2a), but the oscillatory behavior in the HRBS spectra is still preserved. This can also clearly be seen in the results of the RUMP simulation of the spectra (Fig. 2b). From this compositional analysis it is further clear that for all coverages metallic Co grows on top of the Si surface, in addition to diffused-in Co. The diffused-in Co atoms now fill up Si layers which were Co depleted before, but the oscillatory behavior of the Co distribution is still preserved: the 0th and −2nd layers remain depleted of Co at all coverages. The Co contents (Co/Si) in the layers +1 to −3 as obtained from Fig. 2b are plotted in Fig. 2d vs. the evaporated amount of Co (0.1–1.3 ML). The slopes of the plots are indicative of the incorporation rates of Co at and below the surface at different Co coverages. The concentrations of Co in layer 0 and layer −2 are lowest for all coverages. At very initial stages of growth (for 0.1 and 0.36 ML) the amounts of Co in layer 1 and layer 0 stay almost constant, while the amounts of Co in layer −1 and layer −3 strongly increase (see also Fig. 2b). This means that the strong in-diffusion of Co continues at this coverage, leaving the Co content of the surface layer (layer 1) almost unaffected. We would like to note that this is consistent with the suggestions by Horsfield and Fujitani [22] and Peng et al. [23], based on theoretical studies, that bulk diffusion of Co in Si should be very fast, possibly faster than surface diffusion, and the experimental observation of Lee and Bennett [24], who found that bulk diffusion is much faster than surface diffusion at high temperature. Our observations find the same for small coverages even at −60 °C.

For direct comparison with the low temperature growth data presented here, Co HRBS spectra of a sample grown at room temperature [13] (22 °C, measured with 2-MeV N^+ ions, incidence angle 2.5° and scattering angle 37.5°) are presented in Fig. 2c. As the figure shows, the distribution of Co in this sample is markedly different: (i) at −60 °C the Co atoms at the surface occupy positions on top of the Si surface instead of being incorporated in the Si surface, as observed at 22 °C. This

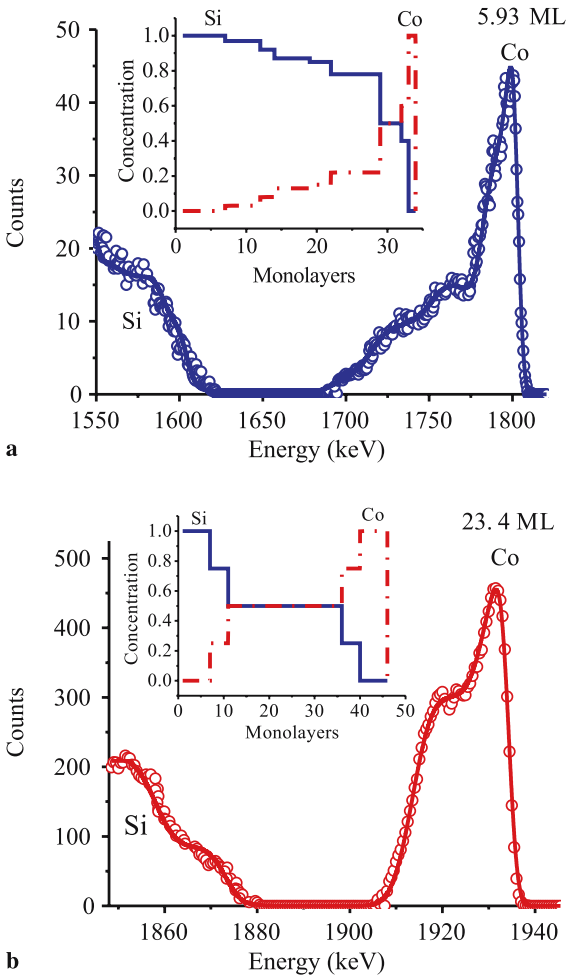

FIGURE 3 HRBS spectra of both the Si and Co edges. (**a**) 5.93 ML of Co deposited at −60 °C and (**b**) 23.42 ML of Co deposited at room temperature (22 °C), together with simulations of the spectra by RUMP (*solid lines* through the data). The *insets* show the Si and Co concentrations at the interface as obtained from the RUMP simulations

results in the formation of a pure Co surface layer at −60 °C instead of the formation of a silicide surface layer at 22 °C. (ii) At −60 °C the in-diffusion of Co is strongly reduced. One can see directly from Fig. 2 that the Co atoms are localized closer to the surface at low temperature than at room temperature. The Co distribution shows a diffusion tail-like envelope at −60 °C which decays rapidly with increasing depth, while at room temperature a two-peak structure is found with surface and subsurface enrichment of Co. (iii) For growth at −60 °C pronounced oscillations in the Co distribution are observed even for coverages above 1 ML (1.3 ML). At room temperature only indications of such oscillations can be seen for very low coverage. Apparently, room temperature is sufficient to distribute the Co atoms more homogeneously over the different Si layers. Besides, at 22 °C, a subsurface maximum in the Co distribution seems to be energetically more favorable.

The consequences of such an inhibited Co in-diffusion at low temperature for the Co/Si interface structure are illustrated in Fig. 3 at higher coverage. There, for direct comparison with low-temperature growth (5.93 ML of Co grown at −60 °C, Fig. 3a), a HRBS spectrum of 23.4 ML of Co grown on Si(100) at room temperature is shown in Fig. 3b. Besides the Co spectra, the high-energy edges of the Si spectra are also shown. For the measurements, beams of 2-MeV N^+ ions (incidence angle 2.5°, Fig. 3a) and 2-MeV He^+ ions (incidence angle 5°, Fig. 3b) were used for −60 °C and 22 °C growth conditions, respectively. The scattering angle was 37.5° in both cases. The RUMP simulations of these spectra are shown as solid lines. (Since we cannot assume a more or less perfect Si lattice with a few Co interstitials at this high coverage, the samples were subdivided into thin sublayers of the thickness of 6.87×10^{14} atoms/cm^2 (Co + Si atoms) in the simulations.) For both cases the Co/Co + Si compositions at the interface are shown in the insets of Fig. 3, as obtained from the RUMP simulations. It is clearly evident that the interface structures at these two temperatures (besides attaining two different coverages) exhibit considerable differences. (i) At −60 °C the interdiffusion of Co and Si is strongly reduced. As a consequence, the growth of pure metallic Co starts much earlier than at 22 °C. At the deposition of 5.93 ML of Co, one monolayer of metallic Co has formed. (ii) The interdiffusion depths of Co and Si seem to be similar for both growth temperatures, but the amount of Co in the silicide phases is much smaller at −60 °C (4.93 ML of Co) than at 22 °C (17.4 ML of Co). (iii) The silicide phases formed at the interface are quite different: at −60 °C only 1 ML of the Co_2Si and 3 ML of the CoSi phases are formed, followed by a long tail of low Co content silicides into the Si bulk. In contrast, at room temperature, well-defined thick silicide layers of higher Co concentrations are formed at the interface: 4 ML of Co_2Si, 25 ML of CoSi and 4 ML of $CoSi_2$. The fraction of stoichiometric CoSi phase formed at the interface is much smaller for −60 °C (1.5 ML of pure Co, corresponding to 30% of the total amount of Co in silicide phases) than for 22 °C (12.5 ML of pure Co, corresponding to 72% of the total amount of Co in silicide phases).

4 Summary

In summary, the Co depth distribution has been measured with monolayer depth resolution in in situ HRBS experiments for Co deposition in the range of 0.1–1.3 ML at −60 °C. At very low coverage Co diffusion into the bulk Si has been observed. The amount of in-diffused Co is, however, less than at room temperature. Also, at −60 °C, Co is the main diffusing species. In contradiction to room-temperature growth, Co atoms form layers of pure Co on top of the Si surface at very low coverage. Every second Si layer, starting with the first Si layer, is Co depleted.

This leads to an oscillatory Co distribution in the Si lattice which is preserved up to higher coverages (1.3 ML). Thus, by low-temperature evaporation we have not only achieved reduced diffusion of Co atoms into the Si lattice, but also reduced out-diffusion of Si, which leads to the growth of metallic Co at the surface right from the beginning. For thicker layers of deposited Co, the low-temperature growth at −60 °C results in the formation of an interface silicide layer with low Co content and only a very thin layer of stoichiometric CoSi composition when compared with room-temperature deposition. There, a thick layer of stoichiometric CoSi is formed.

ACKNOWLEDGEMENTS The authors would like to acknowledge M. Bechtel, Á. Szökefalvi-Nagy and Alaka Tripathy for kind cooperation.

REFERENCES

1 H. Dery, P. Dalal, L. Cywiński, L.J. Sham, Nature **447**, 573 (2007)
2 I. Žutić, J. Fabian, D. Sarma, Rev. Mod. Phys. **76**, 323 (2004)
3 R.J. Soulen, J. Byers, M.S. Osofsky, B. Nadgorny, T. Ambrose, S.F. Cheng, P. Broussard, C.T. Tanaka, J. Nowak, J.S. Moodera, Science **282**, 85 (1998)
4 A.G. Arnov, G.E. Pikus, Sov. Phys. Semicond. **10**, 698 (1976)
5 I. Appelbaum, B. Huang, D.J. Monsma, Nature **447**, 295 (2007)
6 D.R. Loraine, D.I. Pugh, H. Jenniches, R. Kirschman, S.M. Thompson, W. Allen, C. Sirisathikul, J.F. Gregg, J. Appl. Phys. **87**, 5161 (2000)
7 Y.Q. Jia, R.C. Shi, S.Y. Chou, IEEE Trans. Magn. **32**, 4707 (1996)
8 I. Žutić, J. Fabian, Nature **447**, 269 (2007)
9 H.L. Meyerheim, U. Doebler, A. Puschmann, Phys. Rev. B **44**, 5738 (1990)
10 G. Rangelov, P. Augustin, J. Stober, T. Fauster, Phys. Rev. B **49**, 7535 (1994)
11 V. Scheuch, B. Voigtländer, H.P. Bonzel, Surf. Sci. **372**, 71 (1997)
12 M.V. Gomoyunova, I.I. Pronin, N.R. Gall, S.L. Molodsov, D.V. Vyalikh, Tech. Phys. Lett. **29**, 496 (2003)
13 S.P. Dash, D. Goll, H.D. Carstanjen, Appl. Phys. Lett. **90**, 132 109 (2007)
14 K.N. Tu, Appl. Phys. Lett. **27**, 145 (1975)
15 A.P. Horsfield, S.D. Kenny, H. Fujitani, Phys. Rev. B **64**, 245 332 (2001)
16 J.M. Gallego, R. Miranda, S. Molodtsov, C. Laubschat, G. Kaindl, Surf. Sci. **239**, 203 (1990)
17 T. Enders, M. Rilli, H.D. Carstanjen, Nucl. Instrum. Methods Phys. Res. B **136**, 1183 (1992)
18 R. Doolittle, M.O. Thompson, RUMP, Computer Graphics Service (2002)
19 K. Kimura, K. Ohshima, M. Mannami, Phys. Rev. B **52**, 5737 (1995)
20 Y. Chang, J.L. Erskine, Phys. Rev. B **26**, 4766 (1982)
21 H. Reichert, P.J. Eng, H. Dosch, I.K. Robinson, Phys. Rev. Lett. **74**, 2006 (1995)
22 A.P. Horsfield, H. Fujitani, Phys. Rev. B **63**, 235 303 (2001)
23 G.W. Peng, A.C.H. Huan, E.S. Tok, Y.P. Feng, Phys. Rev. B **74**, 195 335 (2006)
24 M.Y. Lee, P.A. Bennett, Phys. Rev. Lett. **75**, 4460 (1995)